



## OPEN ACCESS

## EDITED BY

Tania Martins-Marques,  
University of Coimbra, Portugal

## REVIEWED BY

Xiaojuan Guo,  
Capital Medical University, China  
Zhu Zhang,  
China-Japan Friendship  
Hospital, China

## \*CORRESPONDENCE

Rubin Tan  
tanrubin11@126.com

†These authors have contributed  
equally to this work

## SPECIALTY SECTION

This article was submitted to  
General Cardiovascular Medicine,  
a section of the journal  
Frontiers in Cardiovascular Medicine

RECEIVED 17 May 2022

ACCEPTED 15 November 2022

PUBLISHED 30 November 2022

## CITATION

Tan R, You Q, Yu D, Xiao C,  
Adu-Amankwaah J, Cui J and Zhang T  
(2022) Novel hub genes associated  
with pulmonary artery remodeling in  
pulmonary hypertension.  
*Front. Cardiovasc. Med.* 9:945854.  
doi: 10.3389/fcvm.2022.945854

## COPYRIGHT

© 2022 Tan, You, Yu, Xiao,  
Adu-Amankwaah, Cui and Zhang. This  
is an open-access article distributed  
under the terms of the [Creative  
Commons Attribution License \(CC BY\)](#).  
The use, distribution or reproduction  
in other forums is permitted, provided  
the original author(s) and the copyright  
owner(s) are credited and that the  
original publication in this journal is  
cited, in accordance with accepted  
academic practice. No use, distribution  
or reproduction is permitted which  
does not comply with these terms.

# Novel hub genes associated with pulmonary artery remodeling in pulmonary hypertension

Rubin Tan<sup>1\*†</sup>, Qiang You<sup>2†</sup>, Dongdong Yu<sup>3,4,5</sup>, Chushu Xiao<sup>4,5</sup>, Joseph Adu-Amankwaah<sup>1</sup>, Jie Cui<sup>1</sup> and Ting Zhang<sup>4,5</sup>

<sup>1</sup>Department of Physiology, Basic Medical School, Xuzhou Medical University, Xuzhou, China,

<sup>2</sup>School of Pharmacy, Shandong University of Traditional Chinese Medicine, Jinan, Shandong,

China, <sup>3</sup>Department of Tumor Radiotherapy, Renmin Hospital of Wuhan University, Wuhan, China,

<sup>4</sup>Department of Pathophysiology, School of Basic Medicine, Huazhong University of Science and

Technology, Wuhan, China, <sup>5</sup>Key Laboratory of Pulmonary Diseases of Ministry of Health, Tongji

Medical College, Huazhong University of Science and Technology, Wuhan, China

Pulmonary hypertension (PH) is a life-threatening disease with complex pathogenesis. According to etiology, PH is divided into five major groups in clinical classification. However, pulmonary artery (PA) remodeling is their common feature, in addition to bone morphogenetic protein receptor type 2; it is elusive whether there are other novel common genes and similar underlying mechanisms. To identify novel common hub genes involved in PA remodeling at different PH groups, we analyzed mRNA-Seq data located in the general gene expression profile GSE130391 utilizing bioinformatics technology. This database contains PA samples from different PH groups of hospitalized patients with chronic thromboembolic pulmonary hypertension (CTEPH), idiopathic pulmonary artery hypertension (IPAH), and PA samples from organ donors without known pulmonary vascular diseases as control. We screened 22 hub genes that affect PA remodeling, most of which have not been reported in PH. We verified the top 10 common hub genes in hypoxia with Sugen-induced PAH rat models by qRT-PCR. The three upregulated candidate genes are *WASF1*, *ARHGEF1* and *RB1* and the seven downregulated candidate genes are *IL1R1*, *RHOB*, *DAPK1*, *TNFAIP6*, *PKN1*, *PLOD2*, and *MYOF*. *WASF1*, *ARHGEF1*, and *RB1* were upregulated significantly in hypoxia with Sugen-induced PAH, while *IL1R1*, *DAPK1*, and *TNFAIP6* were upregulated significantly in hypoxia with Sugen-induced PAH. The DEGs detected by mRNA-Seq in hospitalized patients with PH are different from those in animal models. This study will provide some novel target genes to further study PH mechanisms and treatment.

## KEYWORDS

pulmonary hypertension, idiopathic pulmonary artery hypertension, chronic thromboembolic pulmonary hypertension, pulmonary artery remodeling, bioinformatic analysis

## Introduction

Pulmonary hypertension (PH) is a multifaceted disease with a high mortality rate and a low cure rate, characterized by remodeling of the pulmonary artery (PA), which leads to elevated mean pulmonary artery pressure (mPAP), increased pulmonary vascular resistance (PVR), and eventually result in right heart failure (1, 2). According to WHO, PH can be divided into five categories based on pathological features, hemodynamic characteristics, clinical diagnosis, and treatment strategies (3, 4). Although the etiology of PH varies, PA remodeling is a common feature in different groups of PH. The injured pulmonary artery endothelial cells (PAECs) and the phenotype conversion of pulmonary artery smooth muscle cells (PASMCs), which are characterized by excessive proliferation and apoptosis resistance, play vital roles in PA remodeling. Also, the activation of fibroblasts causes the hypersecretion of extracellular matrices, such as collagen, resulting in extracellular matrix deposition, and subsequently, contributing to pulmonary vascular remodeling. Taken together, alterations in the aforementioned cells play three important roles in pulmonary vascular remodeling that contributes to the progression of PH (1–4).

One typical example of common genes is bone morphogenetic protein receptor type 2 (BMPR2), which was first revealed in patients with hereditary PAH and patients with IPAH (5–7), and then validated in the development of group 3 PH (8), chronic thromboembolic pulmonary hypertension (8, 9), valvular heart disease complicated with pulmonary artery hypertension (10), and hypoxia-induced animal model (11, 12). However, the other novel common genes and mechanisms of PA remodeling in different groups of PH are not fully elucidated; hence, it is vital to explore its pathogenesis further. With the development of gene chip technology, the database of gene expression profiles has grown dramatically. There have been some genetic bioinformatics studies utilizing the samples of patients with PH and animal models; most of them are focus studies on a single group of PH, such as idiopathic pulmonary artery hypertension (IPAH, Group 1) (13–16), hypoxia-induced pulmonary hypertension (Group 3) (17), and chronic thromboembolic pulmonary hypertension (CTEPH, Group 4) (18, 19). However, there are few reports on the comparative analysis among different groups of PH.

Some scientists used samples including blood (20, 21) or lung tissue samples (13–18, 22, 23) to indirectly explore genetic changes in PA remodeling. Recently, Gorr et al. identified DEGs between PASMCs derived from patients with IPAH and normal, and they were not sure whether it applies to other PH groups (24). Halliday et al. and Wang et al. directly used human PA as the research object and identified DEGs between CTEPH and the normal groups (18, 19). The common DEGs of PH in different groups have

TABLE 1 Detailed data of GSE130391.

Sequence number of chip	GSE130391
Platform	GPL570
Disease	PH (IPAH and CTEPH)
Chip provider	Pulmonary Lab of Medicine of Vanderbilt University
Address	4200 E 9TH Ave, Box B133, Nashville, TN, USA
Research object	Human
Sample type	Pulmonary artery
Number of chip samples	4 normal, 4 IPAH, 14 CTEPH
Time of uploading chip	Apr 29, 2019

received less attention. Therefore, it is vital to further explore the common genes that are involved in the pathogenesis of PH.

In this study, GSE130391 chip data were selected as the research object, including the gene chip data of pulmonary arteries of organ donors without known pulmonary vascular diseases, patients with IPAH, and patients with CTEPH. First, we compared the differences and similarities between IPAH and CTEPH and screened their common DEGs. Furthermore, the screened common DEGs were verified using hypoxia with Sugden-induced PAH (Group 1).

## Materials and methods

### Bioinformatic analysis

The datasets of gene expression profiles with sequence numbers of GSE130391 were downloaded from the Gene Expression Omnibus (GEO) database, affiliated with the National Center for Biotechnology Information (NCBI) (25, 26), using the *geoquery* package; the details of the chips are listed in Table 1. The *limma* package in R software (version 3.6.3) (University of California, Berkeley, CA) was used to analyze the DEGs between the two groups (27, 28). The *ComplexHeatmap* package in R software was subsequently used to plot the heatmap of the DEGs (29).

Gene ontology enrichment (GO) and KEGG (Kyoto Encyclopedia of Genes and Genomes) pathway analyses of DEGs were performed *via* R software (version 3.6.3) (statistical analysis and visualization). The *clusterProfiler* package was primarily used for enrichment analysis (30); *Org.hs.eg.db* package (version 3.10.0) was used for ID conversion (31). GO analysis consists of biological processes (BP), cellular components (CC), and molecular functions (MF).

The PPI network of DEGs was constructed using STRING (<https://string-db.org/>, cut-off >0.4) (32). The significant modules (MCODE, degree cut-off = 2, node score cut-off = 0.2) and the hub genes were identified using Cytoscape software

(33, 34). The gene expression level and protein expression scores were from the Human Protein Atlas (HPA) database and the Bgee database.

## Hypoxia with Sugen-induced PH model

Adult male Sprague Dawley rats (180–200 g, 8 weeks old) were supplied by the Laboratory Animal Center of Tongji Medical College, Huazhong University of Science and Technology (HUST). The animal study protocol was reviewed and permitted by HUST Animal Care and Use Committee and conducted following the Guidelines for the Care and Use of Laboratory Animals (S1821). They were injected with 20 mg/kg Sugen 5416 (HY-10374, MCE) subcutaneously and exposed to 10% oxygen for 2 weeks; control rats were injected with vehicle (0.5% carboxymethylcellulose, 0.9% NaCl, 0.4% polysorbate, and 0.9% benzyl alcohol in deionized water) (35). As we recently described, hemodynamic studies were performed (35–39). At the end of hemodynamic experiments, the rats were euthanized with anesthetics, the lungs and heart tissues were collected, and a part of the lung was soaked in a formaldehyde solution (4%) for 24 h. The right ventricular hypertrophy was quantified by weighing the right ventricular free wall (RV) and the left ventricle (LV) together with the septum (S, LV+S) (35–39). The rest of the lungs were stored at  $-80^{\circ}\text{C}$  for further analysis. Five-micrometer-thick sections of the lung embedded with paraffin were used to assess PA remodeling after HE-stained. As described in our previous studies, the wall thickness in PAs was determined to be around 50–100  $\mu\text{m}$  diameters (35–39).

## Real-time quantitative RT-PCR

The pulmonary arteries were isolated from the third branch of the intralobular artery in the lung of rat models as described in our previous publications (35–39). RNA extraction (ratio of OD at 260 nm/280 nm > 1.7) was conducted using the Trizol method (15596026, Invitrogen) and reversely transcribed into cDNA according to the manufacturer's recommendations (RR037A, Takara). Candidate primers for each gene of interest were designed using the Premier 5 design program (VertMarkets, Inc., Pennsylvania). The best candidate primers were then selected using BLAST alignment. PCR reaction was performed with the quantitative TB Green-based PCR kit (RR420A, Takara) using a CFX Connect PCR machine (CFX Connect TM, BIO-RAD). The following conditions were set for the reaction: pre-denaturation stage:  $95^{\circ}\text{C}$ , 1 min/1 cycle; amplification stage: denaturation at  $95^{\circ}\text{C}$  for 5 s and annealing at  $58^{\circ}\text{C}$  for 30 s, 40 cycles; melting curve stage:  $65$ – $95^{\circ}\text{C}$ , increment of  $0.5^{\circ}\text{C}$  for 5 s. Results were analyzed using the  $2^{-\Delta\Delta\text{CT}}$

TABLE 2 The q-PCR primer of top 10 hub common DEGs.

Target gene	q-PCR primer
IL1R1 (rat)	F: 5'-CTGCCGAGGCTTGTGACATCTTC-3' R: 5'-CGACAGCAGAGGCACAATGAGAC-3'
RHOB (rat)	F: 5'-CATCCGCAAGAAGCTGGTGGTG-3' R: 5'-TCGGGGAACCTGCTCTTACTGAAC-3'
DAPK1 (rat)	F: 5'-CGACAGCAGAGGCACAATGAGAC-3' R: 5'-GCTCCTCACGCTCACATTCTCAC-3'
TNFAIP6 (rat)	F: 5'-GACGATGTCCACGGCTTTGTAGG-3' R: 5'-ACGGACGCATCACTCAGAACTTC-3'
PKN1 (rat)	F: 5'-ACCTTCCCAGACCATCCCTTG-3' R: 5'-TGAGGTGCTCCGTCCTAAG-3'
PLOD2 (rat)	F: 5'-CGTCTGGCTTCACTTTATCCGAGAG-3' R: 5'-TACGAAGTTCAGCAGGGCAAATCC-3'
MYOF (rat)	F: 5'-GCCTAGAGAAGCAGAAGCACAGTG-3' R: 5'-AGCAGCGTAGGTGGTAGATGTAGAC-3'
WASF1 (rat)	F: 5'-ACAAGTCTGCCTGCCTCTGAG-3' R: 5'-CTTCTGTTCACGCTGCTCTTC-3'
ARHGEF1 (rat)	F: 5'-CCTGAGCCTGGAGATGATGGAGAG-3' R: 5'-TGCCGTTCACTTGGTTCTTG-3'
RB1 (rat)	F: 5'-CCTCCTCTCCAGAGTAACCACAC-3' R: 5'-GTATGGAAGGCTGAGGCTGCTTG-3'

method (40, 41). The primer sequences for each gene are listed in Table 2.

## Western blot

Total proteins were extracted from PAs in control rat models using RIPA lysis buffer containing PMSF and phosphatase inhibitors. Proteins (30  $\mu\text{g}$ /well) were electrophoresed using a 10% sodium dodecyl sulfate (SDS) polyacrylamide gel, as described in our previous studies (39, 42), and transferred to PVDF membranes (Millipore, Germany). The membranes were blocked with 3% BSA for 2 h at room temperature and then incubated with anti-RB1 antibody (1:500, R22869, ZEN BIO, China), anti-ARHGEF1 antibody (1:500, PB10045, BOSTER, China), anti-WASF1 antibody (1:500, R26102, ZEN BIO, China), and anti- $\beta$ -actin (1:10,000, A01010, Abbkine, China) overnight. Bands were detected with ECL Substrate (34580, Thermo Scientific). Integrated density analysis was performed with ImageJ software.

## Statistical analysis

Data are the mean  $\pm$  SE and t-test (and non-parametric tests) was used for two-group comparisons.  $p < 0.05$  represents significant differences.

## Results

### Identification and comparison of DEGs between IPAH and CTEPH

A total of 1,305 differential genes were screened between normal and IPAH subjects, including 617 genes with upregulated expression and 688 with downregulated expression, which was statistically significant ( $|\log_2FC| > 1$ , adj.  $p < 0.05$ ), as illustrated in the volcano map (Figure 1A). A total of 306 differential genes were screened between normal and CTEPH, including 155 genes with upregulated expression and 151 with downregulated expression, which was statistically significant ( $|\log_2FC| > 1$ , adj.  $p < 0.05$ ), as depicted in the volcano map (Figure 1B). Seventy-six overlapping genes with downregulated expression and 44 overlapping genes with upregulated expression were common for IPAH and CTEPH (Figure 1C). However, if the expressions are not distinguished, there are 123 common DEGs in total as shown in Figure 1C. This result shows that three differential genes (*GTF2H2B*, *FOS*, and *FAM114A1*) are upregulated in one group and downregulated in the other group (Figures 1C,D). The general transcription factor II H subunit 2B (*GTF2H2B*) was upregulated in IPAH ( $\log_2FC = 2.60$ , adj.  $p = 0.0001$ ), but downregulated in CTEPH ( $\log_2FC = -1.28$ , adj.  $p = 0.0144$ ). Fos proto-oncogene, AP-1 transcription factor subunit (*FOS*) was downregulated in IPAH ( $\log_2FC = -1.92$ , adj.  $p = 0.0008$ ), but upregulated in CTEPH ( $\log_2FC = 2.99$ , adj.  $p = 0.0003$ ) as Wang et al. reported (19). Family with sequence similarity 114 member A1 (*FAM114A1*) was downregulated in IPAH ( $\log_2FC = -1.03$ , adj.  $p = 0.0234$ ), but upregulated in CTEPH ( $\log_2FC = 1.06$ , adj.  $p = 0.0033$ ).

### Biological features between IPAH and CTEPH

To investigate the biological features of the DEGs, we applied the GO analysis. There were 488 results relative to IPAH, which included 474 BPs, 8 CCs, and 6 MFs. The top five of each ontology that changed are shown in Figure 2A. Regarding BPs of the DEGs of IPAH, these included: significant enrichment in the cellular response to interferon-gamma, response to interferon-gamma, positive regulation of cell–cell adhesion, cellular response to cadmium ion, and regulation of leukocyte cell–cell adhesion (Figures 2A,B; adj.  $p < 0.05$  and  $q < 0.2$ ). Regarding CCs of the DEGs of IPAH, these included: significant enrichment in the nuclear membrane, nuclear outer membrane, external side of the plasma membrane, nuclear envelope, and nuclear inner membrane (Figures 2A,B; adj.  $p < 0.05$  and  $q < 0.2$ ). Regarding MFs of the DEGs of IPAH, these included: significant enrichment in cytokine receptor activity, cytokine receptor binding, cytokine binding, cytokine activity, and tumor necrosis factor receptor superfamily binding (Figures 2A,B; adj.

$p < 0.05$  and  $q < 0.2$ ). These results mainly indicated that some DEGs' products on the nuclear membrane are involved in the cellular response to interferon-gamma in IPAH through binding cytokine-related proteins.

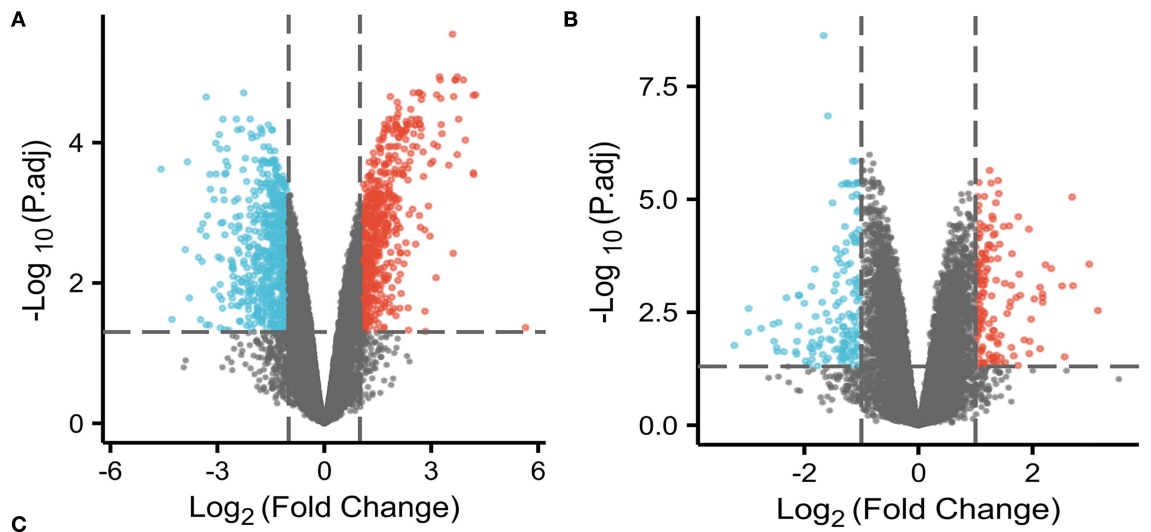
GO analysis identified 58 results in CTEPH, including 50 BPs and 8 MFs. The changes in BPs of DEGs included: enrichment in cellular responses to oxidative stress, calcium ion homeostasis, regulation of actin filament-based processes, myeloid dendritic cell differentiation, and responses to hypoxia (Figures 2C,D; adj.  $p < 0.05$  and  $q < 0.2$ ). The changes in MF of the DEGs included: significant enrichment in L-ascorbic acid binding, phosphatidylinositol binding, enhancer sequence-specific DNA binding, ferrous iron binding, and enhancer binding, as shown in Figures 2C,D. These results suggested that some of the DEG products are involved in oxidative stress, calcium ion homeostasis, and responses to hypoxia in CTEPH through binding phosphatidylinositol proteins.

We also found 22 overlapping functional annotations in IPAH and CTEPH (Figure 2E). They mainly included regulation of actin filament-based process, regulation of inflammatory response, response to oxidative stress, and positive regulation of extracellular matrix organization (Figure 2F). There have been numerous studies related to these biological processes involved in IPAH and CTEPH.

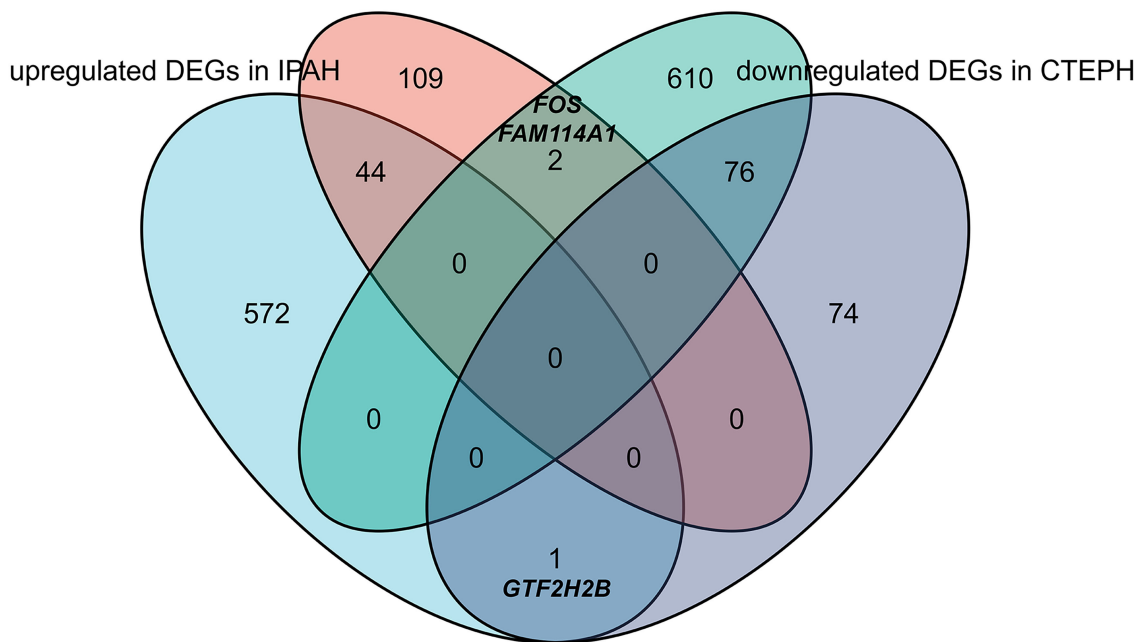
### Possible mechanisms between IPAH and CTEPH

To investigate the possible mechanisms of these DEGs, a KEGG pathway analysis indicated that the DEGs of IPAH were involved in the NF- $\kappa$ B signaling pathway, cytokine–cytokine receptor interaction, osteoclast differentiation, the TNF (tumor necrosis factor) signaling pathway, the C-type lectin receptor signaling pathway, human T-cell leukemia virus 1 infection, viral protein interaction with cytokine and cytokine receptor, and Th17 cell differentiation, under the conditions of adj.  $p < 0.05$  and  $q < 0.2$  (Figures 3A,B). There was no pathway identified under the conditions of adj.  $p < 0.05$  and  $q < 0.2$  in DEGs of CTEPH. However, when the threshold was gene count  $> 2$  and  $p < 0.05$ , the pathway was majorly enriched in cytokine–cytokine receptor interactions; osteoclast differentiation; human T-cell leukemia virus 1 infection; Cushing syndrome; the relaxin signaling pathway; parathyroid hormone synthesis, secretion, and action; insulin secretion; and leishmaniasis (Figure 3C). There are five overlapping pathways (osteoclast differentiation, human T-cell leukemia virus 1 infection, cytokine–cytokine receptor interaction, leishmaniasis, and relaxin signaling pathway) in IPAH and CTEPH. GO and KEGG analysis showed that their PA remodelings share some mechanisms.





upregulated DEGs in CTEPH      downregulated DEGs in IPAH



D

Gene	Description	IPAH		CTEPH	
		Log <sub>2</sub> FC	adj.p	Log <sub>2</sub> FC	adj.p
<i>GTF2H2B</i>	general transcription factor II H subunit 2B	2.6	0.0001	-1.28	0.0144
<i>FOS</i>	Fos proto-oncogene, AP-1 transcription factor subunit	-1.92	0.0008	2.99	0.0003
<i>FAM114A1</i>	Family with sequence similarity 114 member A1	-1.03	0.0234	1.06	0.0033

FIGURE 1

Identification and comparative analysis of DEGs in IPAH and CTEPH. (A,B) Volcano plot analysis identifying DEGs. Red denotes upregulated gene and blue signifies downregulated gene from PA samples from patients with IPAH and CTEPH ( $|\log_{2}FC| > 1$ , adj.  $p < 0.05$ ). (C) Downregulated and upregulated DEGs overlap between IPAH and CTEPH by the bioinformatic analysis were illustrated in the Venn diagram. (D) The detail of three special overlapping DEGs between IPAH and CTEPH.

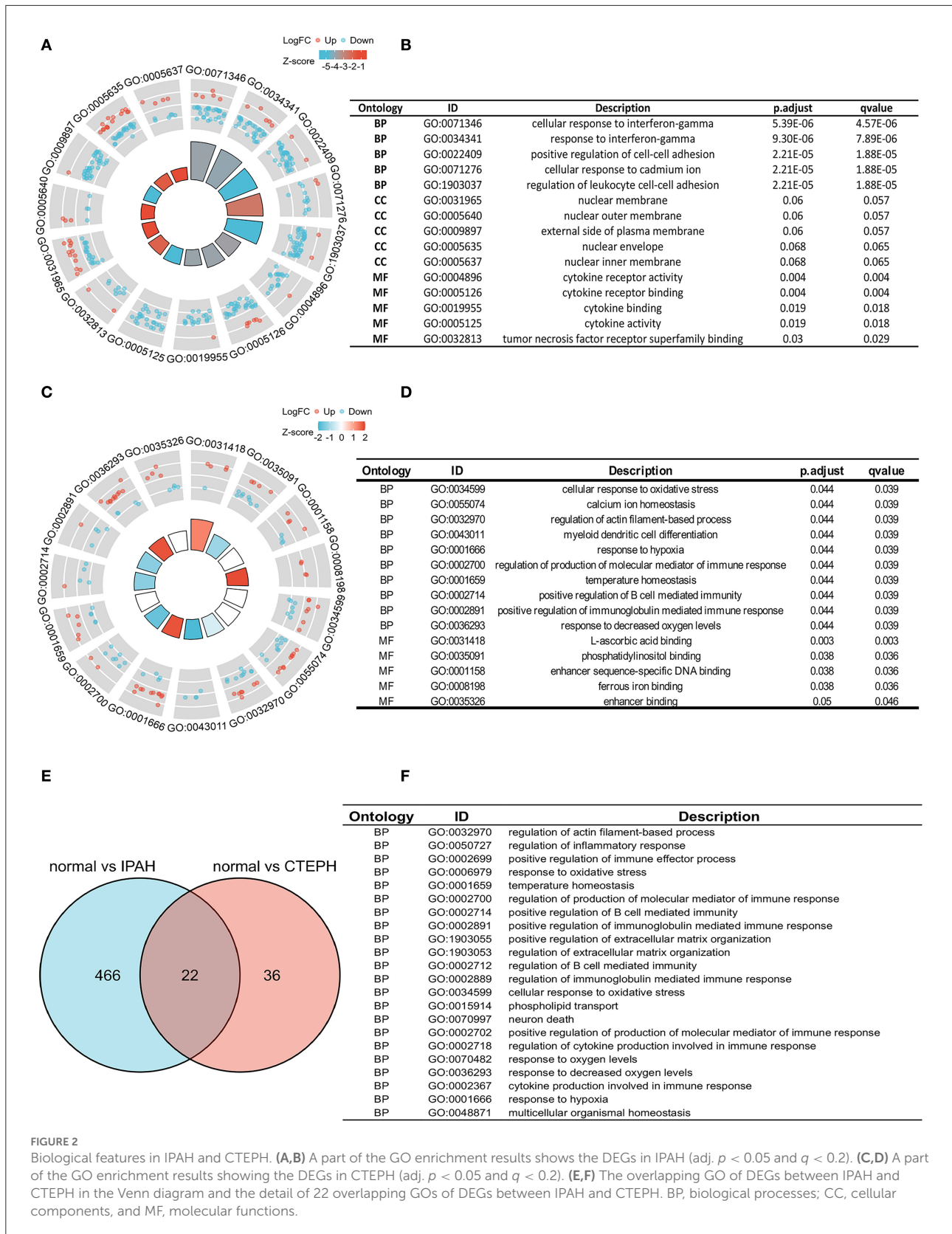
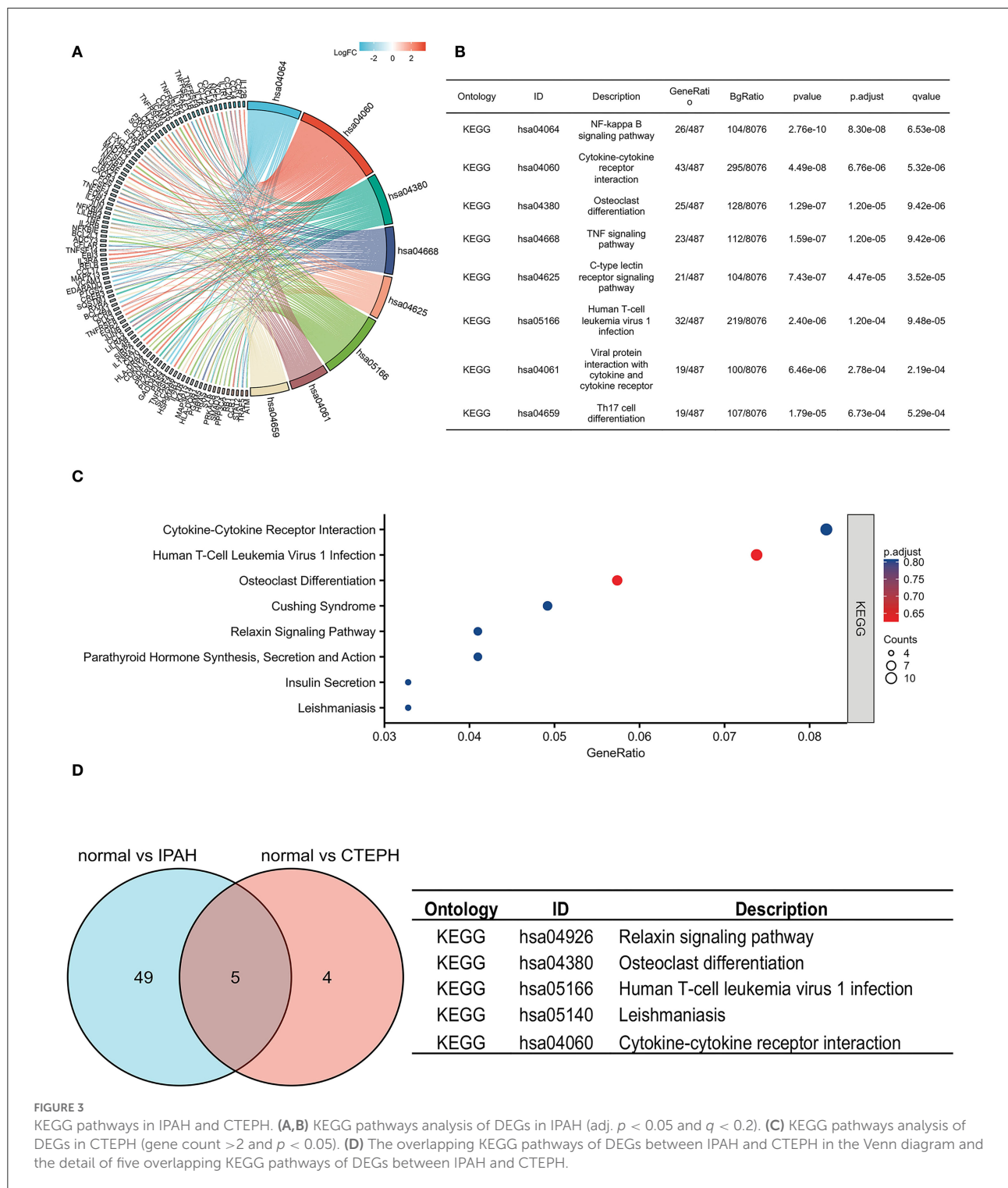


FIGURE 2

Biological features in IPAH and CTEPH. (A,B) A part of the GO enrichment results shows the DEGs in IPAH (adj.  $p < 0.05$  and  $q < 0.2$ ). (C,D) A part of the GO enrichment results showing the DEGs in CTEPH (adj.  $p < 0.05$  and  $q < 0.2$ ). (E,F) The overlapping GO of DEGs between IPAH and CTEPH in the Venn diagram and the detail of 22 overlapping GOs of DEGs between IPAH and CTEPH. BP, biological processes; CC, cellular components, and MF, molecular functions.



### The top 10 hub genes between IPAH and CTEPH

The PPI network of DEGs in IPAH is shown on the left of Figure 4A. The top 10 hub genes include *TNF*,

*IL1B*, *HRAS*, *JUN*, *CCXL8*, *CD40*, *CCND1*, *ICAM1*, *NFKBIA*, and *CD86* (Figure 4A, right; Table 3). The PPI network of DEGs in CTEPH is shown on the left of Figure 4B. The top 10 hub genes included five downregulated genes (*IL4*, *TGFBI*, *SOX9*, *CCL4*, and *EPAS1*) and five upregulated genes

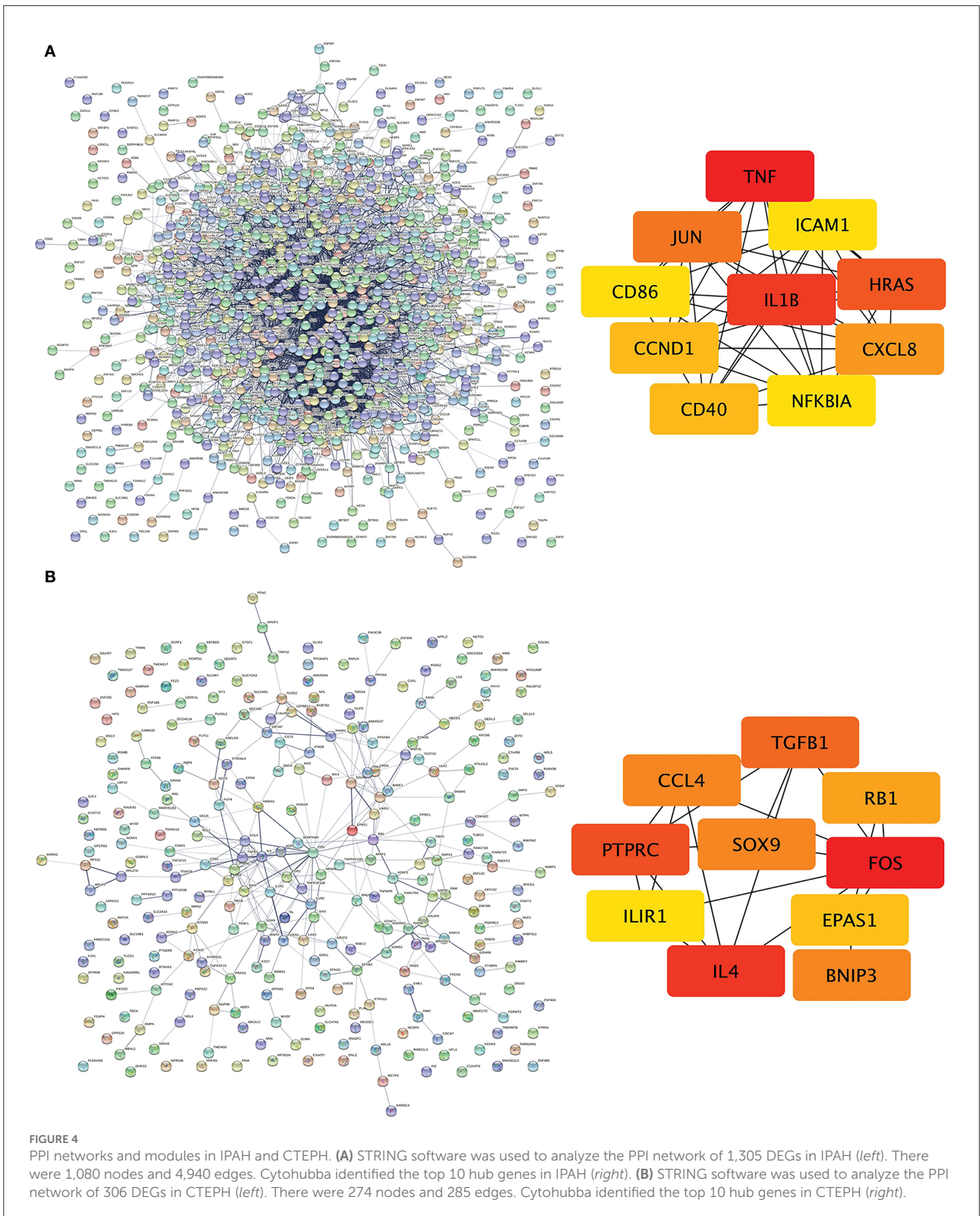




TABLE 3 Top 10 hub genes in IPAH.

Gene	Description	Degree of connectivity	IPAH (logFC)
TNF	Tumor necrosis factor	146	-1.76752525
IL1B	Interleukin 1 beta	116	-2.25446375
HRAS	HRas proto-oncogene, GTPase	99	-1.000599
JUN	Jun proto-oncogene, AP-1 transcription factor subunit	94	-1.85835925
CXCL8	C-X-C motif chemokine ligand 8	84	-3.19954825
CD40	CD40 molecule	75	-2.28042175
CCND1	cyclin D1	75	-2.58089625
ICAM1	Intercellular adhesion molecule 1	74	-3.47023425
NFKBIA	NFKB inhibitor alpha	74	-1.80282
CD86	CD86 molecule	74	-1.11225075

(*FOS*, *PTPRC*, *BNIP3*, *RBI*, and *IL1R1*) (Figure 4A, right; Table 4).

## Screening the common DEGs in IPAH and CTEPH

The Venn diagram shows overlapping genes among normal vs. IPAH and normal vs. CTEPH in Figure 1A. Venn diagram showed that 76 common downregulated DEGs and 44 common upregulated DEGs overlapped in IPAH and CTEPH ( $|\logFC| > 1$ , adjusted  $p < 0.05$ ), which means that these genes do not differ between them, shown in the heatmap (Figure 5A). Furthermore, the correlation heat map analyzed the important patterns and relationships among common DEGs by Spearman (Figure 5B).

GO analysis revealed that the common DEGs were chiefly enhanced in the regulation of extracellular matrix organization, Ras GTPase binding, Rho GTPase binding, small GTPase binding, and androgen receptor binding (adj.  $p < 0.05$  and  $q < 0.2$ ), as shown in Figures 5C,D. KEGG pathway analysis showed that the pathway was mainly enhanced in NF- $\kappa$ B signaling pathway, transcriptional misregulation in cancer, osteoclast differentiation, and cytokine-cytokine receptor interactions (Figures 5E,F). Some of these functional features and pathways have been extensively researched in pulmonary hypertension, which corroborated our findings.

The most significant modules are shown in Figure 5G. Based on the Venn diagram, gene expression levels, and scores, we identified and screened the top 22 hub genes by Cytoscape, including seven upregulated genes, *WASF1*, *ARHGEF1*, *RBI*, *ITM2B*, *ADD3*, *APAF1*, and *LIMD1*, and 15 downregulated

TABLE 4 Top 10 hub genes in CTEPH.

Gene	Description	Degree of connectivity	CTEPH (logFC)
FOS	Fos proto-oncogene, AP-1 transcription factor subunit	24	2.994168071
IL4	Interleukin 4	18	-1.0257366
PTPRC	Protein tyrosine phosphatase receptor type C	17	1.226277071
TGFB1	Transforming growth factor beta 1	12	-1.587007571
SOX9	SRY-box transcription factor 9	11	-1.585361429
CCL4	C-C motif chemokine ligand 4	11	-1.301053857
BNIP3	BCL2 interacting protein 3	11	1.159415
RBI	RB transcriptional corepressor 1	10	1.05062846
EPAS1	Endothelial PAS domain protein 1	9	-1.459483393
IL1R1	Interleukin 1 receptor type 1	8	2.485151893

genes, *IL1R1*, *RHOB*, *DAPK1*, *TNFAIP6*, *PKN1*, *PLOD2*, *TRIP10*, *MYOF*, *DRAM1*, *ULK2*, *FSCN1*, *NR2F2*, *PFN2*, *DMPK*, and *LRP12* (Table 5).

We used the HPA database to compare the gene expression levels of these 22 hub genes between the human lung and smooth muscle tissue. This served as a primary reference for determining whether these 22 hub genes were expressed in lung and smooth muscle tissue. The findings revealed that the gene expression of *RHOB*, *DMPK*, *MYOF*, *NR2F2*, *PLOD2*, *TRIP10*, *PFN2*, *LRP12*, *WASF1*, and *ULK2* were lower in the lung compared to the smooth muscle (Figure 6A). We then analyzed the gene expression scores of these 22 hub genes in the lung and the smooth muscle tissue from the Bgee database. All gene expression scores in the lung and the smooth muscle tissue were high (Figure 6B). Among them are many proteins that have not been detected in the lung tissue or the smooth muscle tissue from the HPA database (Figure 6C).

## qRT-PCR verified the top 10 candidate common hub genes

To verify if these top 10 hub genes do contribute to PA remodeling in any PH, we performed qRT-PCR to



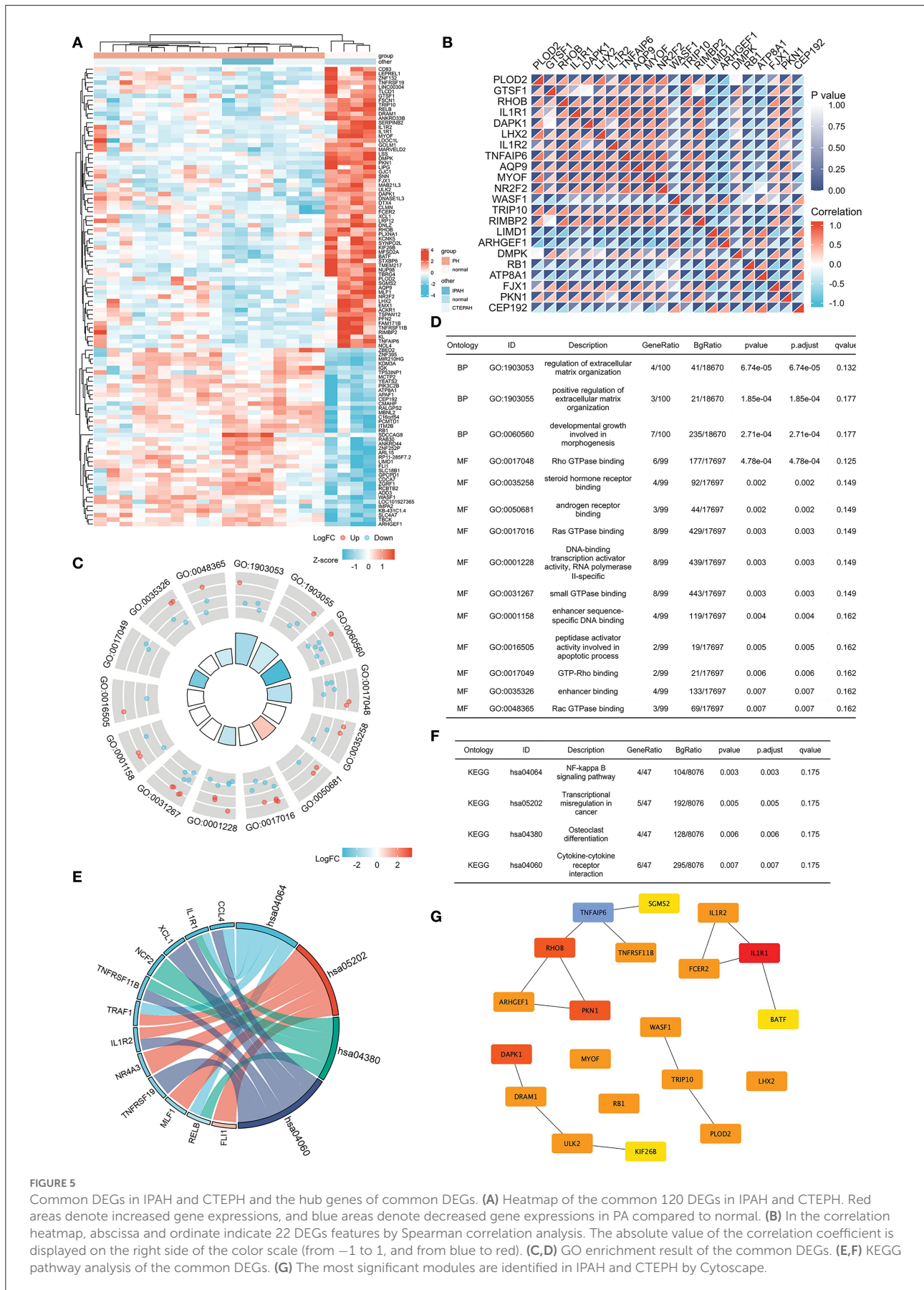


FIGURE 5

Common DEGs in IPAH and CTEPH and the hub genes of common DEGs. (A) Heatmap of the common 120 DEGs in IPAH and CTEPH. Red areas denote increased gene expressions, and blue areas denote decreased gene expressions in PA compared to normal. (B) In the correlation heatmap, abscissa and ordinate indicate 22 DEGs features by Spearman correlation analysis. The absolute value of the correlation coefficient is displayed on the right side of the color scale (from -1 to 1, and from blue to red). (C, D) GO enrichment result of the common DEGs. (E, F) KEGG pathway analysis of the common DEGs. (G) The most significant modules are identified in IPAH and CTEPH by Cytoscape.

TABLE 5 Top 22 hub genes of common DEGs in IPAH and CTEPH.

Gene	Description	Degree of connectivity	IPAH (logFC)	CTEPH (logFC)
IL1R1	Interleukin 1 receptor type 1	4	-3.31181275	-2.485151893
RHOB	Ras homolog family member B	3	-3.429416	-2.315058
DAPK1	Death-associated protein kinase 1	3	-3.03807425	-1.965708857
TNFAIP6	TNF alpha-induced protein 6	3	-2.6127775	-1.741152464
PKN1	Protein kinase N1	3	-1.0623545	-1.105080357
PLOD2	Procollagen-lysine,2-oxoglutarate 5-dioxygenase 2	2	-3.901955	-2.530431857
MYOF	Myoferlin	2	-2.12081	-1.569080464
WASF1	WASP family member 1	2	1.783399	2.03028325
ARHGEF1	Rho guanine nucleotide exchange factor 1	2	1.35552975	1.034979714
RB1	RB transcriptional corepressor 1	2	1.31365525	1.050628464
TRIP10	Thyroid hormone receptor interactor 10	2	-1.630505	-1.284504071
DRAM1	DNA damage regulated autophagy modulator 1	2	-1.5938555	-1.022801571
ULK2	Unc-51 like autophagy activating kinase 2	2	-1.11539675	-1.816644464
ITM2B	Integral membrane protein 2B	1	1.235915286	1.727951
ADD3	Adducin 3	1	2.0188955	1.039967571
APAF1	Apoptotic peptidase activating factor 1	1	1.19376925	1.264531857
LIMD1	LIM domain containing 1	1	1.170496964	1.46983275
FSCN1	Fascin actin-bundling protein 1	1	-2.10963625	-1.261688929
NR2F2	Nuclear receptor subfamily 2 group F member 2	1	-1.8798225	-1.151422321
PFN2	Profilin 2	1	-2.1160365	-1.615431393
DMPK	Dystrophia myotonica-protein kinase	1	-1.35368875	-1.661622036
LRP12	Low density lipoprotein receptor-related protein 12	1	-2.789589	-2.543066786

detect three upregulated candidate genes (*WASF1*, *ARHGEF1*, and *RB1*) and seven downregulated candidate genes (*IL1R1*, *RHOB*, *DAPK1*, *TNFAIP6*, *PKN1*, *PLOD2*, and *MYOF*), using hypoxia with Sugen-induced PAH classified into group 1 (Figure 7).

As shown in Figures 7A–D, in hypoxia with Sugen-induced PH rats (SuHx), mPAP ( $30.00 \pm 0.97$  mmHg for SuHx vs.  $15.46 \pm 1.46$  mmHg for control rats; Figure 7A) and PVR ( $297.06 \pm 11.50$  mmHg min/L for SuHx, vs.  $165.40 \pm 22.50$  mmHg min/L for control rats; Figure 7B) were remarkably elevated. RV/(LV+S) representing right heart hypertrophy increased significantly ( $0.37 \pm 0.01$  for SuHx vs.  $0.28 \pm 0.01$  for control rats; Figure 7C). Pulmonary artery wall thickness representing PA remodeling was significantly increased ( $47.52 \pm 0.67\%$  for SuHx vs.  $29.64 \pm 0.62\%$  for control rats, Figure 7D). qRT-PCR results showed six genes in these 10 common DEGs, which changed significantly after onset (Figure 7E). *WASF1*, *ARHGEF1*, and *RB1* were significantly upregulated, which was consistent with bioinformatics analysis, but *IL1R1*, *DAPK1*, and *TNFAIP6* were significantly upregulated, which was contrary to bioinformatics analysis.

## The protein expression of *WASF1*, *ARHGEF1*, and *RB1*

To further verify the protein expression of *WASF1*, *ARHGEF1*, and *RB1*, we performed a western blot using rat PAs. The protein expression levels of *WASF1* were significantly increased in the hypoxic environment with Sugen-induced PH rats, whereas *ARHGEF1* and *RB1* were significantly decreased in the same hypoxic environment (Figures 8A,B).

## Discussion

Pulmonary artery remodeling is one of the major processes for PH disease, although some characteristics of pulmonary artery remodeling vary in different PH groups. To better understand the mechanism of PA remodeling in the pathogenesis of PH disease, we analyzed the overlapping (common) DEGs associated with PA remodeling from a database containing samples of two PH group patients. By comparing the gene expression profiles between IPAH (Group 1) and CTEPH (Group 4) from the database, we identified

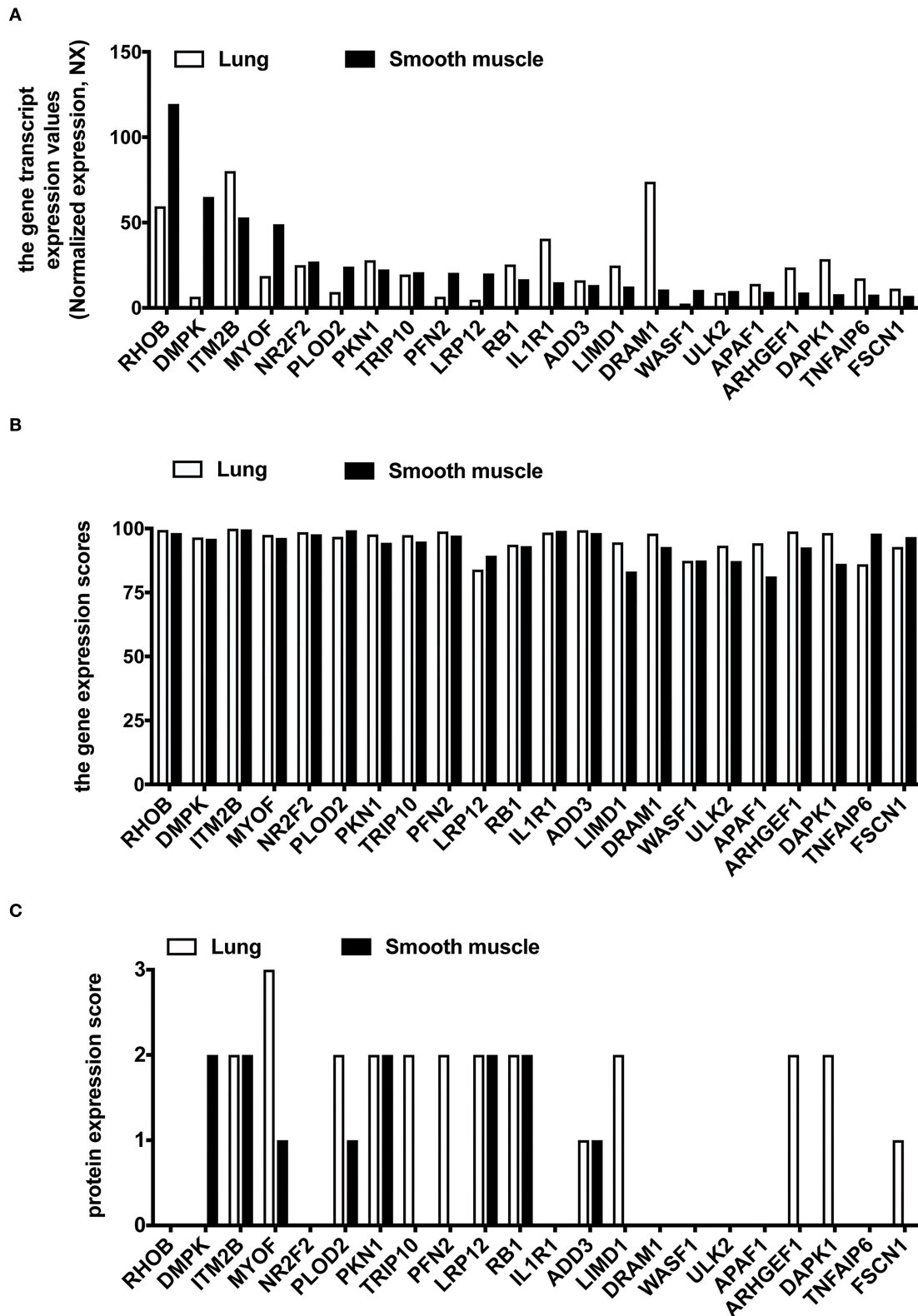
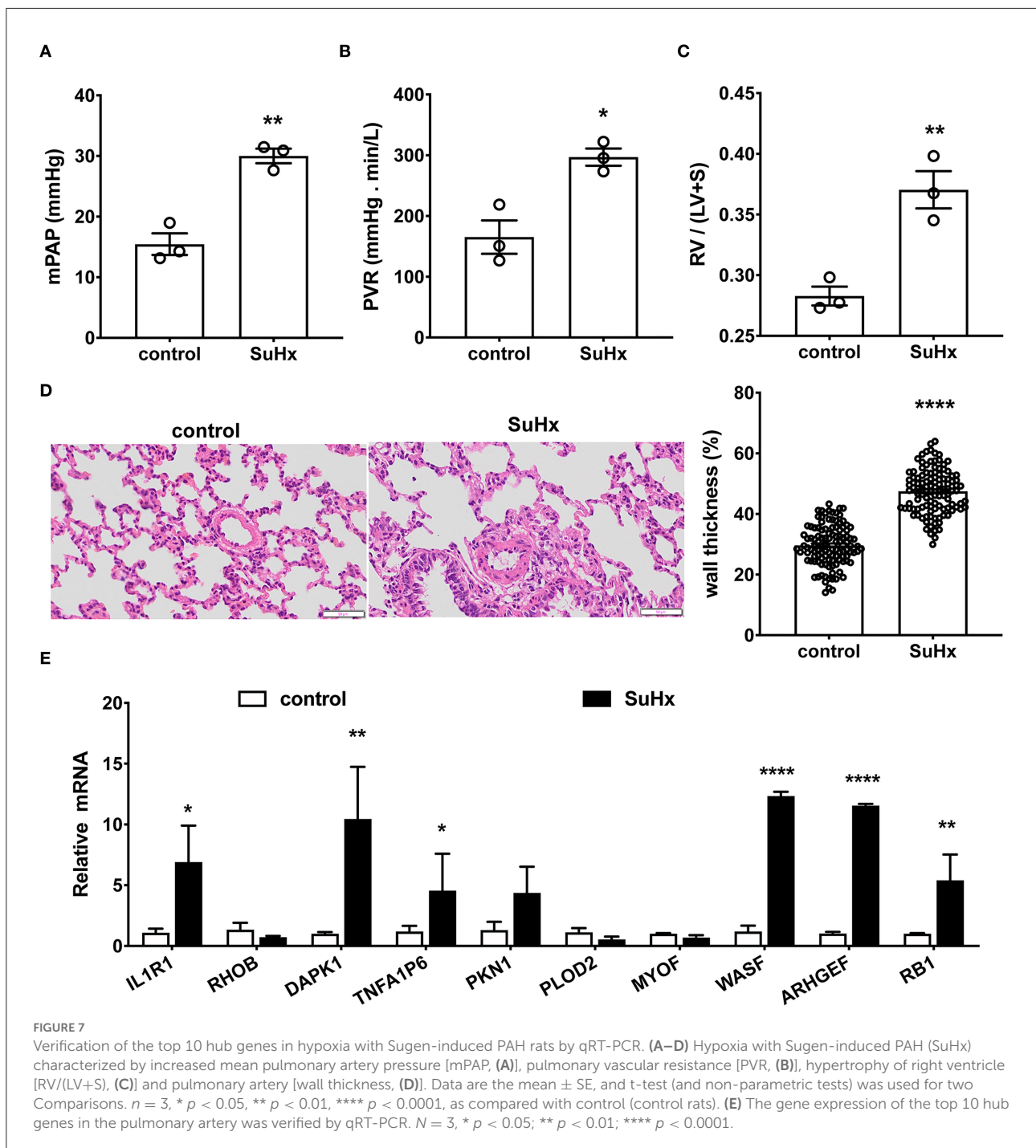


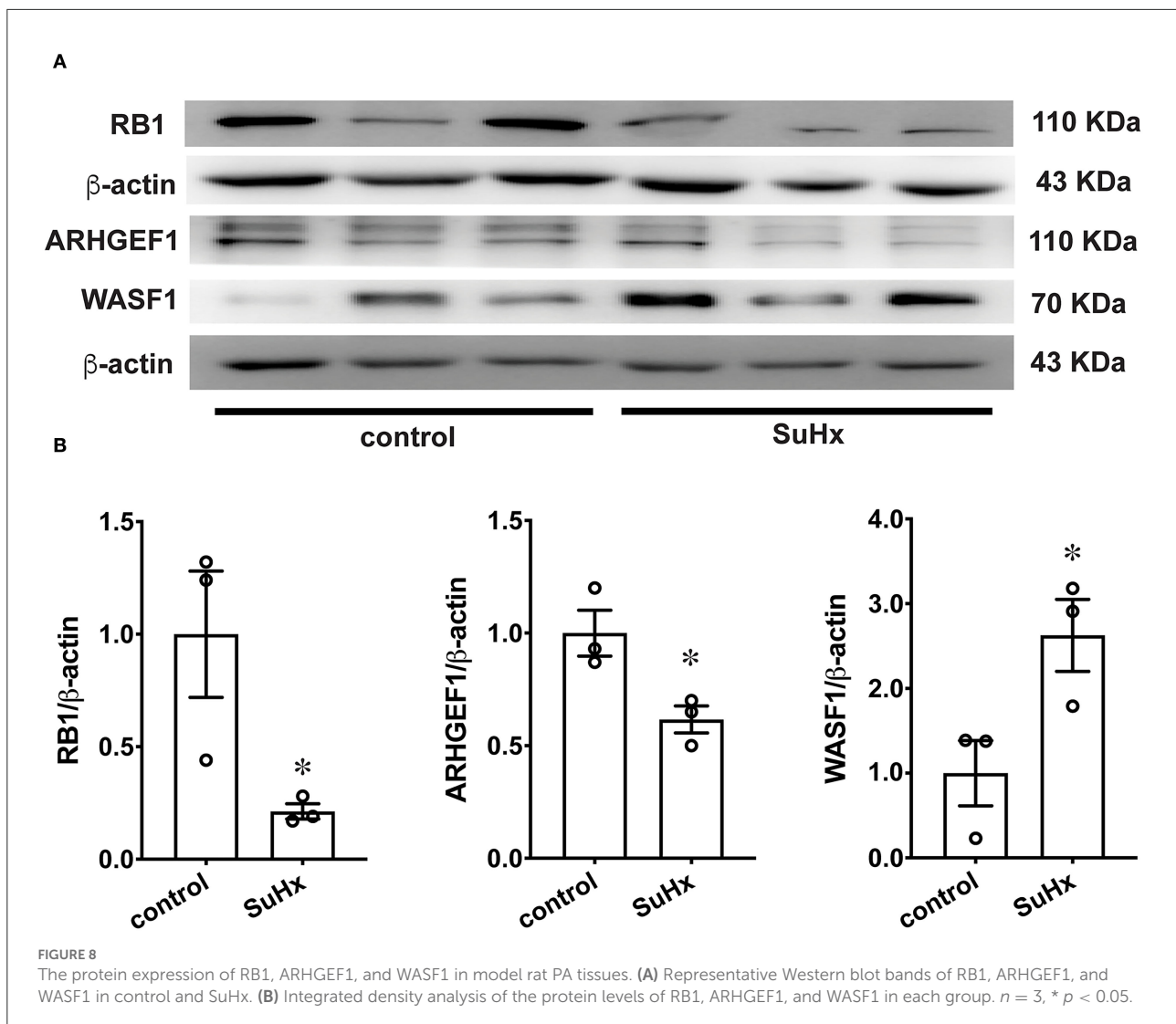
**FIGURE 6**  
The expression analysis of 22 common hub DEGs in human lung and smooth muscle tissues. (A) Gene expression level of hub genes in HPA database. (B) Gene expression scores of hub genes were compared in the Bgee database. (C) Protein expression of hub genes in HPA database.



overlapping sets of DEGs associated with vascular remodeling and enriched signal pathways between them. Among these, there are 76 overlapping genes in downregulated DEGs and 44 in upregulated DEGs between IPAH and CTEPH. Although *GTF2H2B*, *FOS*, and *FAM114A1* are also overlapping genes, they belong to upregulated gene clusters in one group and downregulated gene clusters in other groups. Increased FOS expression in primary PSMCs from patients with CTEPH

was reported to be associated with excessive proliferation and migration of PSMCs (19). Consistently, FOS inhibitors attenuated TNF- $\alpha$  induced proliferation and migration in human PSMCs (19).

Meanwhile, to find out the common mechanisms and hub genes involved in PA remodeling in PH, we screened 22 hub DEGs and verified the top 10 common DEGs by using hypoxia with Sugen-induced PAH rats.



Among the 22 hub genes, it has been reported that *IL1R1* (43–46), *RHOB* (47, 48), *TNFAIP6* (49), *PFN2* (50), and *ARHGEF1* (51, 52) are involved in PA remodeling in different types of PH.

Previous studies have found that inflammation contributed to the development of PH, characterized by a significant increase in serum levels of interleukin (IL)-1 (43). Interleukin (IL)-1 participates in PA remodeling and inflammation during PH by binding to the receptor (IL1R1) which is upregulated and recruiting myeloid differentiation primary response protein 88 (MyD88), which induced IL-1, IL-6, and TNF- $\alpha$  increased through NF- $\kappa$ B activation in patients with IPAH and hypoxia-induced mice (44). IL-1R antagonist protects against murine PH secondary to bronchopulmonary dysplasia (BPD-PH) (45). But IL-1 stimulation reduced collagen expression in PSMCs and parenchymal fibroblasts and subsequently attenuated PA and interstitial remodeling in systemic sclerosis with concomitant

PH (46). Therefore, the role of IL-1 is very complex. IL-1 promotes the proliferation of PASM and parenchymal fibroblasts. However, IL-1 inhibits collagen, and  $\alpha$ -SMA expressions and has direct antifibrotic activity. RhoB (Ras homologous gene family member  $\beta$ ) acts synergistically with RhoA (Ras homologous gene family member  $\alpha$ ) on hypoxia-induced HIF-1 $\alpha$  stability, vascular cell proliferation, and migration *in vitro*. It helps to maximize the continuous hypoxic pulmonary vasoconstriction response and PA remodeling in hypoxia-induced PH and other forms of PH (47, 48). ARHGEF1 (Rho guanine nucleotide exchange factor 1) is related to cytoskeleton structure, microtubule, and the actin cytoskeleton. Recently, it has been described as RhoA-specific nucleotide exchange factor. It catalyzes the exchange of GDP and GTP to produce activated RhoA and participates in the regulation of RhoA activity (49, 50). Tong et al. used the gene expression profile GSE22356 to develop early biomarkers to distinguish



systemic sclerosis with or without PH from the normal population using bioinformatics approaches. They found that *TNFAIP6* (TNF- $\alpha$ -stimulated gene-6) as a hub gene showed an obvious positive correlation between systemic sclerosis with PH (51). Miao et al. (52) also used the gene expression profile GSE130391 to identify five key immune cell-related DEGs, including *PFN2* (profilin 2), in the PA of patients with CTEPH.

*PLOD2* (53), *FSCN1* (54), and *NR2F2* (55) were suggested to play an essential role in the normal development of lung and pulmonary vessels. In addition to these reported genes, six upregulated genes (*WASF1*, *RB1*, *ITM2B*, *ADD3*, *APAF1*, and *LIMD1*) and eight downregulated candidate genes (*DAPK1*, *PKN1*, *TRIP10*, *DRAM1*, *ULK2*, *DMPK*, *LPR12*, and *MYOF*) in PH have not been reported yet.

Some of those genes were randomly selected for verification in two types of rat PH models. Our qRT-PCR results indicated that Wiskott–Aldrich syndrome protein-family 1 (*WASF1*) and *RB1* are significantly upregulated in rat PAH models. The downstream effector molecule, *WASF1*, is implicated in the transmission of signals from small GTPases and tyrosine kinase receptors to the actin cytoskeleton; it also enhances the actin filaments formation (56) and is an important pro-autophagic protein capable of augmenting cell survival (57). *LIMD1* is widely expressed in the lungs, according to Fagerberg et al. (58); this gene encodes an adapter or scaffold protein called LIM domain-containing protein 1 that is involved in the formation of a large number of protein complexes and multiple cellular functions, including gene transcription suppression, cytoskeletal structure, cell fate determination, cell–cell adhesion, cell differentiation, migration, and proliferation (59–64). Furthermore, *LIMD1* functions as a hypoxic regulator by connecting the gap between prolyl hydroxylases and VHL, allowing for effective hypoxia-induced factor 1A (HIF1A) degradation (60). When phosphorylated by CDK3/cyclin-C, *RB1* is a major regulator of cell division and works as a tumor suppressor, promoting the G0-G1 transition. *LIMD1* binds to phosphorylated *RB1*, interacts with E2F1, and inhibits E2F1's transcriptional activity, causing cell cycle arrest (64). Myoferlin (*MYOF*) is a calcium/phospholipid-binding protein involved in muscle growth and repair (65, 66). *MYOF* functions in migration, proliferation, and nitric oxide (NO) release, which occurs in response to vascular endothelial growth factor (VEGF) in endothelial cells (67, 68). According to the function of these genes, we can speculate that they may be involved in vascular cell proliferation, migration, and vascular remodeling.

qPCR results showed that mRNA expression of some DEGs was consistent with mRNA-Seq, and the expression trend of *IL1R1*, *DAPK1*, and *TNFAIP6* genes in animal models was inconsistent with the mRNA-Seq results. One possible reason is that the materials used for data analysis and model validation come from two different species. The materials used in the sequencing database are PAs from patients with PH, and the

material used for PCR verification are PAs from the PH rat model. Although the expression profiles of some genes are similar in two different species, some other genes may have different expression trends. In addition, due to the complex pathogenesis of PH, the gene expression patterns of some genes may be different in different individuals. Evidence showed that the mRNA expression of *IL1R1* (44) and *TNFAIP6* (69) are upregulated in patients with IPAH by validation from qPCR. consistently, *IL1R1* (44) is upregulated in monocrotaline-induced PH rats. These results are consistent with our qPCR results from hypoxia with Sugen-induced PH rats. Western blot analysis showed that ARHGEF1 and *RB1* are decreased in hypoxia with Sugen-induced PH rats. Their protein expression levels are opposite to the gene expression levels, possibly due to post-translational modifications such as degradation by ubiquitination.

Pathway analysis revealed that the NF- $\kappa$ B signaling pathway, osteoclast differentiation, and the regulation of cytokine–cytokine receptor interaction were their common pathways. These functional features and pathways have been widely confirmed in different PH, suggesting that these genes are involved in PA remodeling in PH. From the function and research results of these genes, we can speculate that they must be related to PA remodeling. Thus, due to their key roles in the PA, alterations in their expression may contribute to the development of IPAH and CTEPH.

Although different PH groups share PA remodeling-associated overlapping genes, each group of PH disease has specific pathogenesis. In 2020, Halliday et al. compared the morphology of human PA among CTEPH and IPAH and the control group and found significant differences among them. The expression of all markers in PAECs and PSMCs of CTEPH was generally lower (18). They speculate that it may be caused by cell dedifferentiation (18). In this study, the non-overlapping DEGs may represent the key factors in the different pathogenesis of CTEPH and IPAH.

## Conclusion

This study identified the DEGs and 10 hub genes of IPAH and CTEPH, and 22 hub genes of 120 common DEGs in IPAH and CTEPH using bioinformatics analysis. These results provide the most up-to-date information regarding mechanism research and potential treatment strategies for PA remodeling-related diseases, such as IPAH, CTEPH, and related diseases. However, this study has a limitation, that is, our data could not be interpreted with regard to age, sex, or race due to insufficient sample size. Nevertheless, this study will provide some new target genes for further study of PH mechanisms and treatment.

## Data availability statement

The original contributions presented in the study are included in the article/supplementary material, further inquiries can be directed to the corresponding author/s.

## Ethics statement

The animal study was reviewed and approved by Huazhong University of Science and Technology (HUST) Animal Care and Use Committee, and conducted following the Guidelines for the Care and Use of Laboratory Animals (S1821).

## Author contributions

Conceptualization and experimental design: RT. Experiments, data collection and analysis, and review and editing: RT and QY. Experiments, data analysis, and editing: DY, CX, JC, and TZ. Original draft preparation and data analysis: RT and JA-A. All authors contributed to the article and approved the submitted version.

## Funding

This research was funded by the National Natural Science Foundation of China (81700055), the Outstanding Talent

## References

- Hemnes AR, Humbert M. Pathobiology of pulmonary arterial hypertension: understanding the roads less travelled. *Eur Respir Rev.* (2017) 26:pii:170093. doi: 10.1183/16000617.0093-2017
- Tuder RM, Archer SL, Dorfmueller P, Erzurum SC, Guignabert C, Michelakis E, et al. Relevant issues in the pathology and pathobiology of pulmonary hypertension. *J Am Coll Cardiol.* (2013) 62 (Suppl25):D4–D12. doi: 10.1016/j.jacc.2013.10.025
- Simonneau G, Montani D, Celermajer DS, Denton CP, Gatzoulis MA, Krowka M, et al. Haemodynamic definitions and updated clinical classification of pulmonary hypertension. *Eur Respir J.* (2019) 53:1801913. doi: 10.1183/13993003.01913-2018
- Dodson MW, Brown LM, Elliott CG. Pulmonary arterial hypertension. *Heart Fail Clin.* (2018) 14:255–69. doi: 10.1016/j.hfc.2018.02.003
- Lane KB, Machado RD, Pauculo MW, Thomson JR, Phillips JA 3rd, Loyd JE, et al. Heterozygous germline mutations in BMPR2, encoding a TGF-beta receptor, cause familial primary pulmonary hypertension. *Nat Genet.* (2000) 26:81–4. doi: 10.1038/79226
- Deng Z, Morse JH, Slager SL, Cuervo N, Moore KJ, Venetos G, et al. Familial primary pulmonary hypertension (gene PPH1) is caused by mutations in the bone morphogenetic protein receptor-II gene. *Am J Hum Genet.* (2000) 67:737–44. doi: 10.1086/303059
- Thomson JR, Machado RD, Pauculo MW, Morgan NV, Humbert M, Elliott GC, et al. Sporadic primary pulmonary hypertension is associated with germline

Research Funding of Xuzhou Medical University (Grant No. D2016021), the Natural Science Foundation of Jiangsu Province (BK20160229), and the Natural Science Foundation of the Jiangsu Higher Education Institutions of China (18KJB310017).

## Acknowledgments

The authors thank Dr. Qinghua Hu and Dr. Liping Zhu at Tongji Medical College of Huazhong University of Science and Technology for providing administrative assistance for pulmonary hypertension rats. Additionally, the authors appreciate the contribution of A. Hemnes and J. West toward the availability of GSE130391 from the GEO database.

## Conflict of interest

The authors declare that the research was conducted in the absence of any commercial or financial relationships that could be construed as a potential conflict of interest.

## Publisher's note

All claims expressed in this article are solely those of the authors and do not necessarily represent those of their affiliated organizations, or those of the publisher, the editors and the reviewers. Any product that may be evaluated in this article, or claim that may be made by its manufacturer, is not guaranteed or endorsed by the publisher.

mutations of the gene encoding BMPR-II, a receptor member of the TGF-b family. *J Med Genet.* (2000) 37:741–5. doi: 10.1136/jmg.37.10.741

8. Atkinson C, Stewart S, Upton PD, Machado R, Thomson JR, Trembath RC, et al. Primary pulmonary hypertension is associated with reduced pulmonary vascular expression of type II bone morphogenetic protein receptor. *Circulation.* (2002) 105:1672–8. doi: 10.1161/01.CIR.0000012754.72951.3D

9. Suntharalingam J, Machado RD, Sharples LD, Toshner MR, Sheares KK, Hughes RJ, et al. Demographic features, BMPR2 status and outcomes in distal chronic thromboembolic pulmonary hypertension. *Thorax.* (2007) 62:617–22. doi: 10.1136/thx.2006.070680

10. Li N, Zhu L, Zhu C, Zhou H, Zheng D, Xu G, et al. BMPR2 promoter methylation and its expression in valvular heart disease complicated with pulmonary artery hypertension. *Aging (Albany NY).* (2021) 13:24580–24604. doi: 10.18632/aging.203690

11. Takahashi H, Goto N, Kojima Y, Tsuda Y, Morio Y, Muramatsu M, et al. Downregulation of type II bone morphogenetic protein receptor in hypoxic pulmonary hypertension. *Am J Physiol Lung Cell Mol Physiol.* (2006) 290:L450–8. doi: 10.1152/ajplung.00206.2005

12. Reynolds AM, Xia W, Holmes MD, Hodge SJ, Danilov S, Curiel DT, et al. Bone morphogenetic protein type 2 receptor gene therapy attenuates hypoxic pulmonary hypertension. *Am J Physiol Lung Cell Mol Physiol.* (2007) 292:L1182–92. doi: 10.1152/ajplung.00020.2006

13. Stearman RS, Bui QM, Speyer G, Handen A, Cornelius AR, Graham BB, et al. Systems analysis of the human pulmonary arterial

- hypertension lung transcriptome. *Am J Respir Cell Mol Biol.* (2019) 60:637–49. doi: 10.1165/rcmb.2018-0368OC
14. Xiao G, Zhuang W, Wang T, Lian G, Luo L, Ye C, et al. Transcriptomic analysis identifies Toll-like and Nod-like pathways and necroptosis in pulmonary arterial hypertension. *J Cell Mol Med.* (2020) 24:11409–21. doi: 10.1111/jcmm.15745
  15. Ma Y, Chen SS, Feng YY, Wang HL. Identification of novel biomarkers involved in pulmonary arterial hypertension based on multiple-microarray analysis. *Biosci Rep.* (2020) 40:BSR20202346. doi: 10.1042/BSR20202346
  16. Hemnes AR, Zhao M, West J, Newman JH, Rich S, Archer SL, et al. Critical genomic networks and vasoreactive variants in idiopathic pulmonary arterial hypertension. *Am J Respir Crit Care Med.* (2016) 194:464–75. doi: 10.1164/rccm.201508-1678OC
  17. Hu CJ, Poth JM, Zhang H, Flockton A, Laux A, Kumar S, et al. Suppression of HIF2 signalling attenuates the initiation of hypoxia-induced pulmonary hypertension. *Eur Respir J.* (2019) 54:1900378. doi: 10.1183/13993003.00378-2019
  18. Halliday SJ, Matthews DT, Talati MT, Austin ED, Su YR, Absi TS, et al. A multifaceted investigation into molecular associations of chronic thromboembolic pulmonary hypertension pathogenesis. *JRSM Cardiovasc Dis.* (2020) 9:2048004020906994. doi: 10.1177/2048004020906994
  19. Wang F, Sun C, Lv X, Sun M, Si C, Zhen Y, et al. Identification of a novel gene correlated with vascular smooth muscle cells proliferation and migration in chronic thromboembolic pulmonary hypertension. *Front Physiol.* (2021) 12:744219. doi: 10.3389/fphys.2021.744219
  20. Elinoff JM, Mazer AJ, Cai R, Lu M, Graninger G, Harper B, et al. Meta-analysis of blood genome-wide expression profiling studies in pulmonary arterial hypertension. *Am J Physiol Lung Cell Mol Physiol.* (2020) 318:L98–L111. doi: 10.1152/ajplung.00252.2019
  21. Arwood MJ, Vahabi N, Lteif C, Sharma RK, Machado RF, Duarte JD. Transcriptome-wide analysis associates ID2 expression with combined pre- and post-capillary pulmonary hypertension. *Sci Rep.* (2019) 9:19572. doi: 10.1038/s41598-019-55700-y
  22. Rajkumar R, Konishi K, Richards TJ, Ishizawa DC, Wiechert AC, Kaminski N, et al. Genomewide RNA expression profiling in lung identifies distinct signatures in idiopathic pulmonary arterial hypertension and secondary pulmonary hypertension. *Am J Physiol Heart Circ Physiol.* (2010) 298:H1235–48. doi: 10.1152/ajpheart.00254.2009
  23. Mura M, Cecchini MJ, Joseph M, Granton JT. Osteopontin lung gene expression is a marker of disease severity in pulmonary arterial hypertension. *Respirology.* (2019) 24:1104–10. doi: 10.1111/resp.13557
  24. Gorr MW, Sriram K, Muthusamy A, Insel PA. Transcriptomic analysis of pulmonary artery smooth muscle cells identifies new potential therapeutic targets for idiopathic pulmonary arterial hypertension. *Br J Pharmacol.* (2020) 177:3505–18. doi: 10.1111/bph.15074
  25. Clough E, Barrett T. The gene expression omnibus database. *Methods Mol Biol.* (2016) 1418:93–110. doi: 10.1007/978-1-4939-3578-9\_5
  26. Sean D, Meltzer PS. GEOquery: a bridge between the gene expression omnibus (GEO) and BioConductor. *Bioinformatics.* (2007) 23:1846–7. doi: 10.1093/bioinformatics/btm254
  27. Gordon KS. *Limma: Linear Models for Microarray Data. Bioinformatics and Computational Biology Solutions Using R and Bioconductor.* New York, NY: Springer (2005). p. 397–420.
  28. Ritchie ME, Phipson B, Wu D, Hu Y, Law CW, Shi W, et al. Limma powers differential expression analyses for RNA-seq and microarray studies. *Nucleic Acids Res.* (2015) 43:e47. doi: 10.1093/nar/gkv007
  29. Gu Z, Eils R, Schlesner M. Complex heatmaps reveal patterns and correlations in multidimensional genomic data. *Bioinformatics.* (2016) 32:2847–9. doi: 10.1093/bioinformatics/btw313
  30. Yu G, Wang L G, Han Y, He QY. clusterProfiler: an R package for comparing biological themes among gene clusters. *OMICS.* (2012) 16:284–7. doi: 10.1089/omi.2011.0118
  31. Huang DW, Sherman BT, Lempicki RA. Bioinformatics enrichment tools: paths toward the comprehensive functional analysis of large gene lists. *Nucleic Acids Res.* (2009) 37:1–13. doi: 10.1093/nar/gkn923
  32. Franceschini A, Szklarczyk D, Frankild S, Kuhn M, Simonovic M, Roth A, et al. STRING v9.1: protein-protein interaction networks, with increased coverage and integration. *Nucleic Acids Res.* (2013) 41:D808–15. doi: 10.1093/nar/gks1094
  33. Chin CH, Chen SH, Wu HH, Ho CW, Ko MT, Lin CY. cytoHubba: identifying hub objects and sub-networks from complex interactome. *BMC Syst Biol.* (2014) 8:S11. doi: 10.1186/1752-0509-8-S4-S11
  34. Bandettini WP, Kellman P, Mancini C, Booker OJ, Vasu S, Leung SW, Wilson JR, et al. MultiContrast delayed enhancement (MCOE) improves detection of subendocardial myocardial infarction by late gadolinium enhancement cardiovascular magnetic resonance: a clinical validation study. *J Cardiovasc MagnReson.* (2012) 14:83. doi: 10.1186/1532-429X-14-83
  35. Xiao R, Luo S, Zhang T, Lv Y, Wang T, Zhang J, et al. Peptide blocking self-polymerization of extracellular calcium-sensing receptor attenuates hypoxia-induced pulmonary hypertension. *Hypertension.* (2021) 78:1605–16. doi: 10.1161/HYPERTENSIONAHA.120.16712
  36. Zeng X, Zhu L, Xiao R, Liu B, Sun M, Liu F, et al. Hypoxia-induced mitogenic factor acts as a nonclassical ligand of calcium-sensing receptor, therapeutically exploitable for intermittent hypoxia-induced pulmonary hypertension. *Hypertension.* (2017) 69:844–54. doi: 10.1161/HYPERTENSIONAHA.116.08743
  37. Zhu L, Liu F, Hao Q, Feng T, Chen Z, Luo S, et al. Dietary geranylgeranyl pyrophosphate counteracts the benefits of statin therapy in experimental pulmonary hypertension. *Circulation.* (2021) 143:1775–92. doi: 10.1161/CIRCULATIONAHA.120.046542
  38. Zhu L, Xiao R, Zhang X, Lang Y, Liu F, Yu Z, et al. Spermine on endothelial extracellular vesicles mediates smoking induced pulmonary hypertension partially through calcium-sensing receptor. *Arterioscler Thromb Vasc Biol.* (2019) 39:482–95. doi: 10.1161/ATVBAHA.118.312280
  39. Tan R, Li J, Liu F, Liao P, Ruiz M, Dupuis J, et al. Phenylalanine induces pulmonary hypertension through calcium-sensing receptor activation. *Am J Physiol Lung Cell Mol Physiol.* (2020) 319:L1010–20. doi: 10.1152/ajplung.00215.2020
  40. Tang H, Babicheva A, McDermott KM, Gu Y, Ayon RJ, Song S, et al. Endothelial HIF-2 $\alpha$  contributes to severe pulmonary hypertension due to endothelial-to-mesenchymal transition. *Am J Physiol Lung Cell Mol Physiol.* (2018) 314:L256–75. doi: 10.1152/ajplung.00096.2017
  41. Shen H, Zhang J, Wang C, Jain PP, Xiong M, Shi X, et al. MDM2-mediated ubiquitination of angiotensin-converting enzyme 2 contributes to the development of pulmonary arterial hypertension. *Circulation.* (2020) 142:1190–204. doi: 10.1161/CIRCULATIONAHA.120.048191
  42. Tan R, Li J, Peng X, Zhu L, Cai L, Wang T, et al. GAPDH is critical for superior efficacy of female bone marrow-derived mesenchymal stem cells on pulmonary hypertension. *Cardiovasc Res.* (2013) 100:19–27. doi: 10.1093/cvr/cvt165
  43. Zhang J, Lu X, Liu M, Fan H, Zheng H, Zhang S, et al. Melatonin inhibits inflammasome-associated activation of endothelium and macrophages attenuating pulmonary arterial hypertension. *Cardiovasc Res.* (2020) 116:2156–69. doi: 10.1093/cvr/cvz312
  44. Parpaleix A, Amsellem V, Houssaini A, Abid S, Breau M, Marcos E, et al. Role of interleukin-1 receptor 1/MyD88 signalling in the development and progression of pulmonary hypertension. *Eur Respir J.* (2016) 48:470–83. doi: 10.1183/13993003.01448-2015
  45. Bui CB, Kolodziej M, Lamanna E, Elgass K, Sehgal A, Rudloff I, et al. Interleukin-1 receptor antagonist protects newborn mice against pulmonary hypertension. *Front Immunol.* (2019) 10:1480. doi: 10.3389/fimmu.2019.01480
  46. Birnhuber A, Crnkovic S, Biasin V, Marsh LM, Odler B, Sahu-Osen A, et al. IL-1 receptor blockade skews inflammation towards Th2 in a mouse model of systemic sclerosis. *Eur Respir J.* (2019) 54:1900154. doi: 10.1183/13993003.00154-2019
  47. Duluc L, Ahmetaj-Shala B, Mitchell J, Abdul-Salam VB, Mahomed AS, Aldabbous L, et al. Tipifarnib prevents development of hypoxia-induced pulmonary hypertension. *Cardiovasc Res.* (2017) 113:276–87. doi: 10.1093/cvr/cvw258
  48. Wojciak-Stothard B, Zhao L, Oliver E, Dubois O, Wu Y, Kardassis D, et al. Role of RhoB in the regulation of pulmonary endothelial and smooth muscle cell responses to hypoxia. *Circ Res.* (2012) 110:1423–34. doi: 10.1161/CIRCRESAHA.112.264473
  49. Bear MD, Li M, Liu Y, Giel-Moloney MA, Fanburg BL, Toksoz D. The Lbc Rho guanine nucleotide exchange factor  $\alpha$ -catulin axis functions in serotonin-induced vascular smooth muscle cell mitogenesis and RhoA/ROCK activation. *J Biol Chem.* (2010) 285:32919–26. doi: 10.1074/jbc.M109.062513
  50. Yu L, Quinn DA, Garg HG, Hales CA. Heparin inhibits pulmonary artery smooth muscle cell proliferation through guanine nucleotide exchange factor-H1/RhoA/Rho kinase/p27. *Am J Respir Cell Mol Biol.* (2011) 44:524–30. doi: 10.1165/rcmb.2010-0145OC
  51. Tang Y, Zha L, Zeng X, Yu Z. Identification of biomarkers related to systemic sclerosis with or without pulmonary hypertension using co-expression analysis. *J Comput Biol.* (2020) 27:1519–31. doi: 10.1089/cmb.2019.0492
  52. Miao R, Dong X, Gong J, Wang Y, Guo X, Li Y, et al. Possible immune regulation mechanisms for the progression of

- chronic thromboembolic pulmonary hypertension. *Thromb Res.* (2021) 198:122–31. doi: 10.1016/j.thromres.2020.11.032
53. Sen P, Dharmadhikari AV, Majewski T, Mohammad MA, Kalin TV, Zabielska J, et al. Comparative analyses of lung transcriptomes in patients with alveolar capillary dysplasia with misalignment of pulmonary veins and in foxf1 heterozygous knock-out mice. Comparative study. *PLoS ONE.* (2014) 9:e94390. doi: 10.1371/journal.pone.0094390
54. Kardon G, Ackerman KG, McCulley DJ, Shen Y, Wynn J, Shang L, et al. Congenital diaphragmatic hernias: from genes to mechanisms to therapies. *Dis Model Mech.* (2017) 10:955–70. doi: 10.1242/dmm.028365
55. Pfeffer T, Lignelli E, Inoue H, Mižiková I, Surate Solaligue DE, Steenbock H, et al. Minoxidil cannot be used to target lysyl hydroxylases during postnatal mouse lung development: a cautionary note. *Pharmacol Exp Ther.* (2020) 375:478–87. doi: 10.1124/jpet.120.000138
56. Ozawa M, Hiver S, Yamamoto T, Shibata T, Upadhyayula S, Kiyosue YM, et al. Adherens junction regulates cryptic lamellipodia formation for epithelial cell migration. *J Cell Biol.* (2020) 219:e202006196. doi: 10.1083/jcb.202006196
57. Zhang Z, Wu B, Chai W, Cao L, Wang Y, Yu Y, et al. Knockdown of WAVE1 enhances apoptosis of leukemia cells by downregulating autophagy. *Int J Oncol.* (2016) 48:2647–56. doi: 10.3892/ijo.2016.3446
58. Fagerberg L, Hallström BM, Oksvold P, Kampf C, Djureinovic D, Odeberg J, et al. Analysis of the human tissue-specific expression by genome-wide integration of transcriptomics and antibody-based proteomics. *Mol Cell Proteomics.* (2014) 13:397–406. doi: 10.1074/mcp.M113.035600
59. Kiss H, Kedra D, Yang Y, Kost-Alimova M, Kiss C, O'Brien KP, et al. A novel gene containing LIM domains (LIMD1) is located within the common eliminated region 1 (C3CER1) in 3p21.3. *Human Genet.* (1999) 105:552–9. doi: 10.1007/s004399900188
60. Foxler DE, Bridge KS, Foster JG, Grevitt P, Curry S, Shah KM, et al. A HIF-LIMD1 negative feedback mechanism mitigates the pro-tumorigenic effects of hypoxia. *EMBO Mol Med.* (2018) 10:e8304. doi: 10.15252/emmm.201708304
61. Zeng X, Wang H, He D, Jia W, Ma R. LIMD1 increases the sensitivity of lung adenocarcinoma cells to cisplatin via the GADD45alpha/p38 MAPK signaling pathway. *Front Oncol.* (2020) 10:969. doi: 10.3389/fonc.2020.00969
62. Sharp TV, Al-Attar A, Foxler DE, Ding L, de A Vallim TQ, Zhang Y, et al. The chromosome 3p213-encoded gene, LIMD1, is a critical tumor suppressor involved in human lung cancer development. *Proc Natl Acad Sci USA.* (2008) 105:19932–7. doi: 10.1073/pnas.0805003105
63. Tang J, Zhu L, Huang Y, Shi B, Zhang S, Gu L, et al. Silencing of LIMD1 promotes proliferation and reverses cell adhesion-mediated drug resistance in non-Hodgkin's lymphoma. *Oncol Lett.* (2019) 17:2993–3000. doi: 10.3892/ol.2019.9921
64. Sharp TV, Munoz F, Bourboulia D, Presneau N, Darai E, Wang HW, et al. LIM domains-containing protein 1 (LIMD1), a tumor suppressor encoded at chromosome 3p21.3, binds pRB and represses E2F-driven transcription. *Proc Natl Acad Sci USA.* (2004) 101:16531–6. doi: 10.1073/pnas.0407123101
65. Doherty KR, Demonbreun AR, Wallace GQ, Cave A, Posey AD, Heretis K, et al. The endocytic recycling protein EHD2 interacts with myoferlin to regulate myoblast fusion. *J Biol Chem.* (2008) 283:20252–60. doi: 10.1074/jbc.M802306200
66. Demonbreun AR, Posey AD, Heretis K, Swaggart KA, Earley JU, Pytel P, et al. Myoferlin is required for insulin-like growth factor response and muscle growth. *FASEB J.* (2010) 24:1284–95. doi: 10.1096/fj.09-136309
67. Bernatchez PN, Acevedo L, Fernandez-Hernando C, Murata T, Chalouni C, Kim J, et al. Myoferlin regulates vascular endothelial growth factor receptor-2 stability and function. *J Biol Chem.* (2007) 282:30745–53. doi: 10.1074/jbc.M704798200
68. Zhu W, Zhou B, Zhao C, Ba Z, Xu H, Yan X, et al. Myoferlin, a multifunctional protein in normal cells, has novel and key roles in various cancers. *J Cell Mol Med.* (2019) 23:7180–9. doi: 10.1111/jcmm.14648
69. Lauer ME, Aytikin M, Comhair SA, Loftis J, Tian L, Farver CF, et al. Modification of hyaluronan by heavy chains of inter- $\alpha$ -inhibitor in idiopathic pulmonary arterial hypertension. *J Biol Chem.* (2014) 289:6791–8. doi: 10.1074/jbc.M113.512491